Advances in Pharmacology and Pharmacy 10(4): 253-264, 2022 http://www.hrpub.org
DOI: 10.13189/app.2022.100404

Plant Gum Aided Mucoadhesive Microspheres to Eradicate *Helicobacter pylori* and Its Optimization with Design-Expert's Central Composite Design

Sowjanya Hatthi Belgal Mundarinti[1], Hindustan Abdul Ahad[2,*]

[1]Jawaharlal Nehru Technological University-Anantapur (JNTUA), Ananthapuramu-515001, Andhra Pradesh, India
[2]Department of Industrial Pharmacy, Raghavendra Institute of Pharmaceutical Education and Research (RIPER)-Autonomous, K. R. Palli Cross, Ananthapuramu-515721, Andhra Pradesh, India

Received May 30, 2022; Revised June 30, 2022; Accepted August 23, 2022

Cite This Paper in the Following Citation Styles

(a): *[1] Sowjanya Hatthi Belgal Mundarinti, Hindustan Abdul Ahad , "Plant Gum Aided Mucoadhesive Microspheres to Eradicate Helicobacter pylori and Its Optimization with Design-Expert's Central Composite Design," Advances in Pharmacology and Pharmacy, Vol. 10, No. 4, pp. 253 - 264, 2022. DOI: 10.13189/app.2022.100404.*

(b): *Sowjanya Hatthi Belgal Mundarinti, Hindustan Abdul Ahad (2022). Plant Gum Aided Mucoadhesive Microspheres to Eradicate Helicobacter pylori and Its Optimization with Design-Expert's Central Composite Design. Advances in Pharmacology and Pharmacy, 10(4), 253 - 264. DOI: 10.13189/app.2022.100404.*

Abstract Aim: The aim of the work was to explore the mucoadhesive properties of Mastic gum by involving it in mucoadhesive microspheres with Amoxicillin Trihydrate as a model drug. Using Carbopol-934P and varying amounts of Mastic gum. Methods: 9 interpretations of mucoadhesive microspheres were made by using Design expert software. A central composite design was applied to test the impact of independent variables (Carbopol-934P and mastic gum levels) on drug released at 10h and mucoadhesive strength as the response. Results: A congeniality and physical exam was conducted on the microspheres to see if Amoxicillin Trihydrate (ATH) was present, including its liberation. In formulations that contain lower levels of MG, mucoadhesion strength increased and drug released at the end of 10h was greater. Conclusion: Since MG acts as a release retardant, the amount of drug released is slightly reduced when higher levels are present in formulations. ATH gastro retention for eradicating with Mastic gum aided mucoadhesion (as this gum is proven *H. pylori* activity) is capable of completely capturing the gastrointestinal tract and effectively delivering the medication to the stomach.

Keywords Additive, Amoxicillin, Design Mastic Gum, Mucoadhesive, Microspheres

1. Introduction

There is a rising inclination among drug administrations to expand the availability of drugs through the stomach, with patient acceptance [1]. As a particularly easy-to-prepare and administer dosage form, gastro retentive microspheres are noteworthy [2, 3].

The semi-synthetic aminopenicillin amoxicillin trihydrate (ATH), or oral product containing amoxicillin trihydrate, has broad-spectrum [4] bactericidal activity. ATH is likely to be a white powder, and when given orally [5], it is well absorbed based on its physical, chemical, and biopharmaceutical constraints. Earlier studies have proved that ATH is effective in contradiction of *H. pylori* [6, 7], but its less retention time in the stomach, makes the treatment less effective [6, 8]. So an innovative attempt was made to retain ATH by formulating it as mucoadhesive microspheres.

It is the properties of the polymer used in mucoadhesive systems that make mucoadhesive systems resolute. Several patients prefer the oral route as it is convenient for drug administration. Mucoadhesive drives have been tried with many polymers but are rare and expensive. Searching for a natural polymer that helps mucoadhesion. A study will be conducted by the authors using Mastic gum (MG) to investigate mucoadhesive microspheres. A natural polymer that facilitates

mucoadhesion is preferable to synthetic polymers [9, 10]. Researchers studied mucoadhesive microspheres with MG (Mastic gum). MG has been revealed to have a healing effect on stomach/peptic ulcers and is effective against *H. pylori* [11-13]. The work aiming at ATH mastic gum mucoadhesive microspheres (AMMM) is to reach a steady-state systemic availability in expanded time. Precise liberation systems are a cleverer approach for short t½ drugs and those that need incessant medicating, as they are designed with ease.

Due to the relatively ease of controlling one variable at a time, traditional research focuses on one variable at a time. All these factors cannot be analyzed simultaneously and statistically. It will result in inaccurate results because these factors are interconnected. Multivariate analysis depends heavily on the design of experiments (DOE) [14, 15]. Partially determinable factors are included in the DOE. The objectives of DOE are screening and optimization. Every combination of factors is incorporated into a factorial design (FD) [16]. High levels are either (+1) or low levels (-1) in FD, and these two levels are called FD. To evaluate the response of mucoadhesive microspheres of ATH, design expert software was used.

2. Materials and Methods

Materials

Waksman Selman Pharmaceuticals Pvt. provided the amoxicillin trihydrate. Limited, Anantapur, India. Merck, Hyderabad, provided carbopol 934P, and dichloromethane.

Cleansing of the Mastic gum

MG was cleansed as described by Ahad *et al.,* (2009) and Terpou *et al.,* (2018) with little modifications [17, 18] . MG was defined homogenization as using Biologics-300VT followed by centrifugation (Remi R-8C), neutralization with NaOH, and dialysation (Spectroflo-KR1) with distilled water. Afterward, ethanol (95%) was treated with acetone and diethyl ether until the precipitate was removed.

Experimental design

To optimize the AMMM with Design-Expert software (11.0.5.0, Stat-Ease Inc.), a 9 run, central composite design (CCD) was implemented. With the consequential quadratic model, the key, boundary, and quadratic chattels of independent variables were assessed:

$$Y= B_0+B_1 X_1+B_2X_2+B_{12}X_1X_2+B_1X^2+ B_2X^2$$

Y is the dependent variable, X_1 and X_2 are the independent variables, and B_0, B_1 and B_2 are the regression coefficients of the independent variables (Carbopol 934P and MG). For AMMM, the dependent variables/responses were drug released at 10 h (DR10h) and mucoadhesion strength (g). The authors adopted a central composite design (CCD) experiments to determine the variables and levels used in optimizing the AMMM. The ingredients in various AMMM are listed in Table 1.

Table 1. Composition of the AMMM

Components	Formulation								
	F-1	F-2	F-3	F-4	F-5	F-6	F-7	F-8	F-9
Amoxicillin Trihydrate (mg)	250	250	250	250	250	250	250	250	250
Ethyl Cellulose (mg)	50	50	50	50	50	50	50	50	50
MG (mg)	50	50	50	75	75	75	100	100	100
Carbopol 934P (mg)	50	75	100	50	75	100	50	75	100
Dichloromethane (ml)	30	30	30	30	30	30	30	30	30
Span 80 (minims)	4	4	4	4	4	4	4	4	4
Glutaraldehyde (minims)	4	4	4	4	4	4	4	4	4
Liquid paraffin (ml)	250	250	250	250	250	250	250	250	250

Preparation of AMMM

Acryl acetate (2% v/v), carbopol 934P, and carbopol 934MG were dissolved in dichloromethane. The mixture was continuously stirred into liquid paraffin (containing span 80) using a three-bladed propeller stirrer (IKA-R1385) rotating at 1500 rpm. Dropwise additions of gluteraldehyde were made to the procedure every hour at 4 minim concentrations. The stirring continued for 3h. Centrifugation was used to separate the AMMM (Amoxicillin-Azadirachta indica mucoadhesive microspheres). Before washing with petroleum ether, liquid paraffin was removed. AMMM was suspended with sodium bisulfite 5% v/v in a solution of gluteraldehyde-removing gluteraldehyde for 15 min. The last step was to wash with distilled water. AMMMs were dried and stored using vacuum desiccators [19, 20].

Evaluation parameters

Identification of drug

We compared the sample spectrum of ATH with the reference spectrum for any changes in the functional groups.

Resolving of melting point

By using the open capillary method, the melting point of ATH was determined.

Drug Excipient compatibility studies

DSC

Using a 1:1 ratio mixture of ATH and MG, 10 mg (5 mg per sample) was scanned at 50-300°C using a DSC crucible (Venchal Scientific-412105-USA).

FTIR

FTIR spectroscopy (Bruker) was used to evaluate the synergy between ATH and MG by scanning a 4000-400 cm^{-1} array.

Evaluation of physical properties

Particle Size Measurement

The particle size of the AMMM was controlled on a stage micrometer scale. An ocular microscope was used to count AMMM on a dry slide, and an ocular microscope was used to examine wet AMMM. In each batch, at least 100 AMMM were counted [21].

Production Yield

An estimate of the production yield was based on the ratio of the average weight of parched (eq.1) AMMM (W_1) recovered from each of three trials to the initial dry weight (W_2) [22].

$$\% \text{ Yield } = \frac{\text{Weight of attained by microspheres}}{Total\ weight\ of\ drug\ and\ polymer} \times 100 \quad (1)$$

Entrapment Efficiency

The AMMM (100 mg) were dispersed in 0.1 M HCl overnight with erratic quivering. At 272 nm, the excitation wavelength of the spectrophotometer was used to measure the spectral abundance of the mixture (Elico Spectrophotometer, SL -174). Based on the ratio of the actual amount of the drug present in the formulation to the initial amount, the entrapment efficiency was calculated by eq.2 [23].

$$\text{Entrapment efficacy } = \frac{\text{Practical drug yield}}{Theoritical\ drug\ content} \times 100 \quad (2)$$

Swelling Measurement

To swell the AMMMs, they were kept in 0.1M HCl. Following 3h, the cells were removed, centrifuged, and the weight gained was determined by the difference between the weight gain at time t (Xt) and the initial weight gain (t = 0 [X0]) as determined by the eq. 3 [24].

$$\% \text{ SI } = \frac{X_t - X_0}{X_0} \times 100 \quad (3)$$

Where Xt-weight of the AMMM after time t; Xo- Initial weight of the AMMM

Mucoadhesion Measurement Study

A freshly cut sheep stomach was obtained within 60 min of the animal's death and eviscerated by washing with isotonic saline to determine mucoadhesive strength (MS). On the mucosal surface, an accurate weight of AMMM was installed on a polyethylene plate, which was immobile at a position of 40° relative to the straight plane. A solution of HCl (0.1M) warmed to 37±1°C was applied to the tissue at a rate of 5 ml/min. Visual inspection was used to record the time necessary to detach all the AMMM from the mucosa (eq.4) [25, 26].

$$\text{Force of adhesion (N)} = \\ = \frac{\text{Mucoadhesive strength (g)} \times 9.81}{1000} \times 100 \quad (4)$$

***In Vitro* ATH Release Study**

A dissolution test using the USP-II apparatus at a stirring rate of 50±5 rpm at 370.5°C with 900 ml of HCl (0.1N HCl) as a dissolution medium revealed the *in vitro* release of AMMM. We introverted a 5 ml sample at diverse intervals, and we restocked the volume of the media with the same amount of dissolution media [27, 28]. Following that, samples were spectrophotometrically analyzed at 272nm.

Statistical optimization

To determine the independent influences on retorts, Design-Expert software was employed to calculate contour plots (2D) and response surfaces (3D). ANOVA eatables were used to validate polynomial intentions statistically. Using the ANOVA endowment, a statistical

model was created to discover model multiplication and aptitude. A F-value with a 0.05 significance level. AMMM evaluates MG's congeniality based on the color of the MG, which is yellowish in colour.

3. Results

Identification of drug

The authors compared the sample spectrum of ATH with the reference spectrum and found no significant differences in the functional groups.

Determination of Melting Point

ATH has a melting point in the range of 199.7±3.1°C

Compatibility studies

The DSC analysis determined that pure ATH produced a sharp endothermic peak at 196.52°C and peaked at 200.43°C, indicating that it was pure. When combined with excipients, this peak broadens (peak at 195.51°C). Based on the DSC results, the excipients were not in contact with ATH.

ATH exhibits distinctive peaks characteristic of FTIR bands for secondary amines, distending phenyl esters, and vibrational carboxylic groups. In the meantime, the blend (F-9) was found to be closer to the wavelengths. When measuring ATH with excipients, none of the peaks or stretches in the spectrum were obstructed.

Physical properties

As described in Table 2, the micromeritic observations for AMMM are given.

Particle size

All formulations were measured using optical microscopy. The AMMM array ranges from 35.2±0.9 to 48.1±0.6 μm, among which F-5 has a larger particle size (Table 3).

Yield of AMMM

% Yield for AMMM was 82.2±1.2 to 96.2±2.3, F-4 and F-5 show a maximum (Table 3).

% Drug entrapment

AMMM entraps drugs in the range of 69.1±1.0 to 82.3±0.9, with F-6 and F-4 giving the most entrapment (Table 3).

Swelling Measurement

Swelling was least noticeable in batches F-1, F-2, and F-3, and greatest in batch F-9. Perhaps there is not enough MG in the body to cause swelling. F-7, F-8, and F-9 have the highest concentration of MG (Table 3).

Table 2. Micromeritic properties of AMMM

Formulation	Bulk density	Tapped density	Carr's index	Hausner ratio	Angle of repose (o)
F-1	0.356±0.01	0.386±0.02	7.772± 0.21	1.084±0.02	25.04±0.02
F-2	0.369±0.02	0.395±0.02	6.582± 0.01	1.070±0.03	26.05±0.95
F-3	0.528±0.01	0.558±0.04	5.376± 0.06	1.056±0.02	26.51±0.18
F-4	0.458±0.02	0.469±0.03	2.345± 0.05	1.024±0.01	27.58±0.34
F-5	0.238±0.02	0.252±0.01	5.555± 0.02	1.058±0.01	28.04±0.04
F-6	0.363±0.03	0.378±0.02	3.968± 0.08	1.041±0.04	27.20±0.14
F-7	0.459±0.04	0.476±0.03	3.571± 0.10	1.037±0.02	28.95±0.08
F-8	0.516±0.03	0.532±0.03	3.007± 0.01	1.031±0.01	27.06±0.74
F-9	0.489±0.02	0.511±0.04	4.305± 0.02	1.044±0.01	28.22±0.65

Values in mean ± S.D; trials (n): 3

Table 3. Physical properties of AMMM

Formulation	Particle size (µm)	% Yield	Drug entrapment (%)	Swelling index (%)
F-1	46.3±0.9	88.2±2.5	71.2±2.4	62.5±1.3
F-2	46.8±0.8	87.6±1.7	72.3±2.8	63.8±2.3
F-3	47.9±0.7	88.5±1.0	72.9±0.8	64.4±1.7
F-4	55.8±0.7	92.2±0.5	75.6±1.7	71.6±1.0
F-5	58.4±0.8	94.2±1.6	75.3±2.6	72.8±1.5
F-6	56.2±0.5	93.9±3.3	76.8±1.5	72.9±0.8
F-7	59.6±0.9	89.3±1.5	81.2±0.9	75.6±1.2
F-8	59.8±1.3	90.5±2.2	81.9±0.8	76.1±2.3
F-9	61.7±1.2	91.3±1.5	82.3±2.3	76.5±1.5

Values in mean ± S.D; trials (n): 3

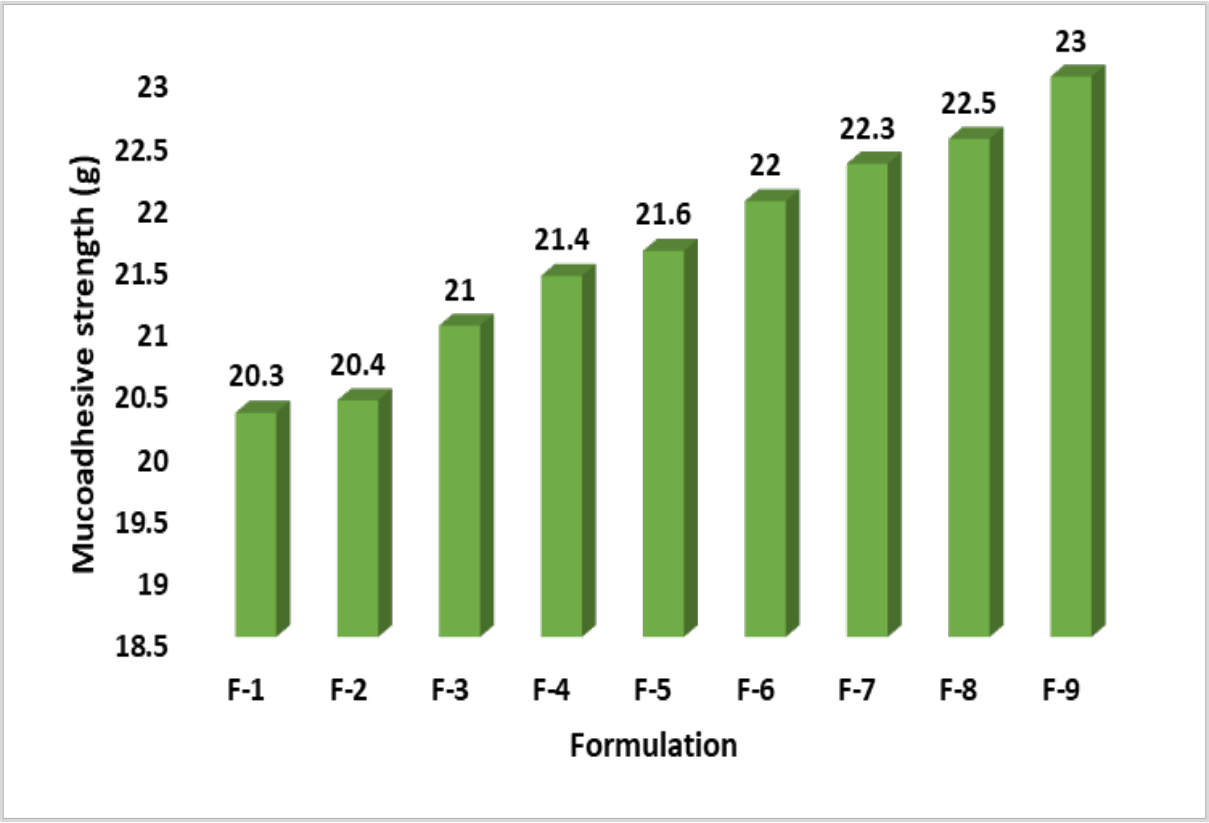

Figure 1. Mucoadhesive strength for the AMMM

In vitro mucoadhesion

The % mucoadhesion of all batches of AMMM were perceived to be in the array of 20.3g (F-1) to 23g (F-9) (Fig. 1). Higher MG content was associated with greater mucoadhesion.

In vitro drug release

AMMM was studied *in vitro* for dissolution. Compared to formulations F-1 and F-2, formulations F-1 and F-2 exhibit the highest amount of ATH release (Fig. 2) at the end of the 10-h testing period.

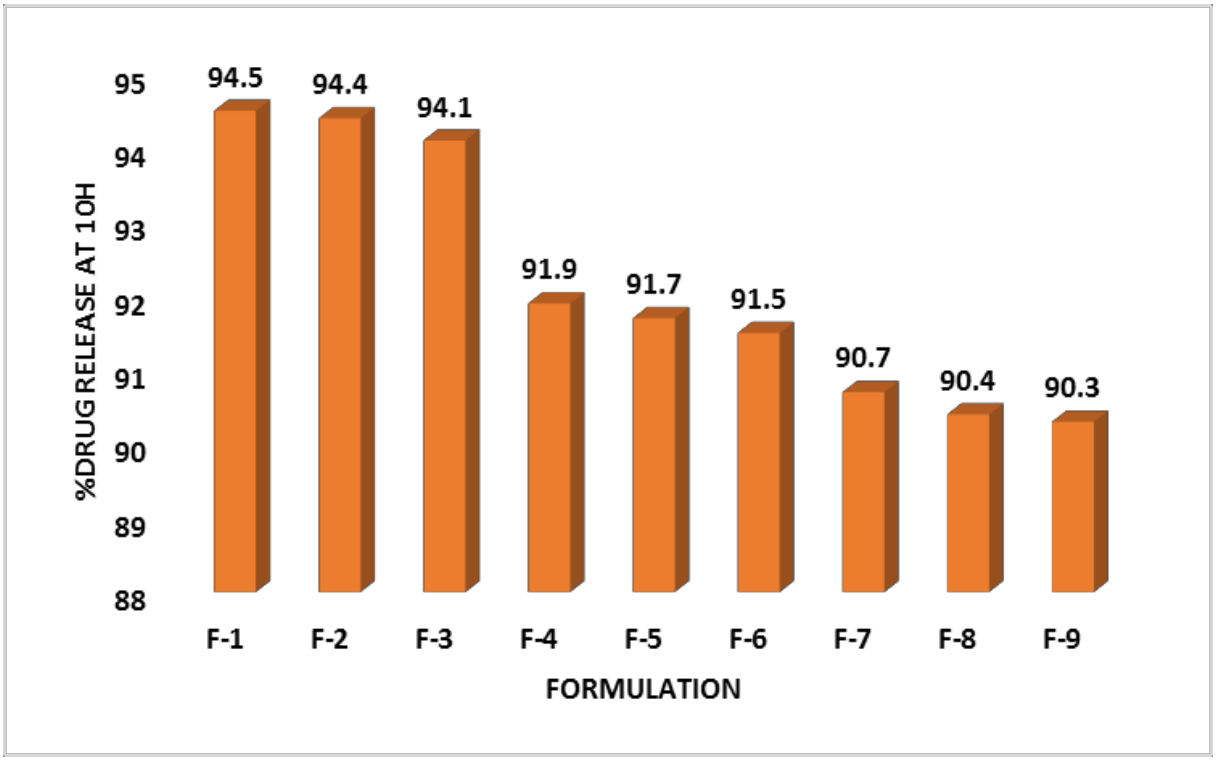

Figure 2. Drug released at 10th h from AMMM

Table 4. Summary of regression values of various kinetic release models

Formulation	Zero order	First order	Higuchi	Korsmeyer Peppas	Hixson Crowell
	R^2				
F-1	0.9512	0.9036	0.9012	0.9141	0.9248
F-2	0.9589	0.9135	0.9225	0.9356	0.9226
F-3	0.9599	0.9036	0.9101	0.9456	0.9158
F-4	0.9652	0.9251	0.9107	0.9249	0.9365
F-5	0.9689	0.9037	0.9215	0.9264	0.9324
F-6	0.9698	0.8916	0.9128	0.9208	0.9319
F-7	0.9456	0.9126	0.9168	0.9165	0.9294
F-8	0.9428	0.9125	0.9254	0.9017	0.9264
F-9	0.9419	0.9102	0.9245	0.9056	0.9258

ATH estimation and release kinetics

With a UV-VIS spectrometer, a calibration curve was obtained at λ_{max} 272 nm for ATH estimation in 0.1M HCl solution. Beer's law witnessed to building the calibration curve was in the array of 0-10 µg/ml (repeated thrice). This data helps in determining content uniformity.

According to AMMM, zero-order kinetics best fit the release kinetics. The ATH release track for the linear kinetic procedure is shown in Table 4.

Diagnostic analysis

Diagnostic analysis for DR10h

Diagnostic plots were used to evaluate the goodness of fit of the DR10h (Fig. 3A–D).

Diagnostic analysis for mucoadhesive strength

A diagnostic plot was used to verify the goodness of fit of the MS (Fig. 3E–H).

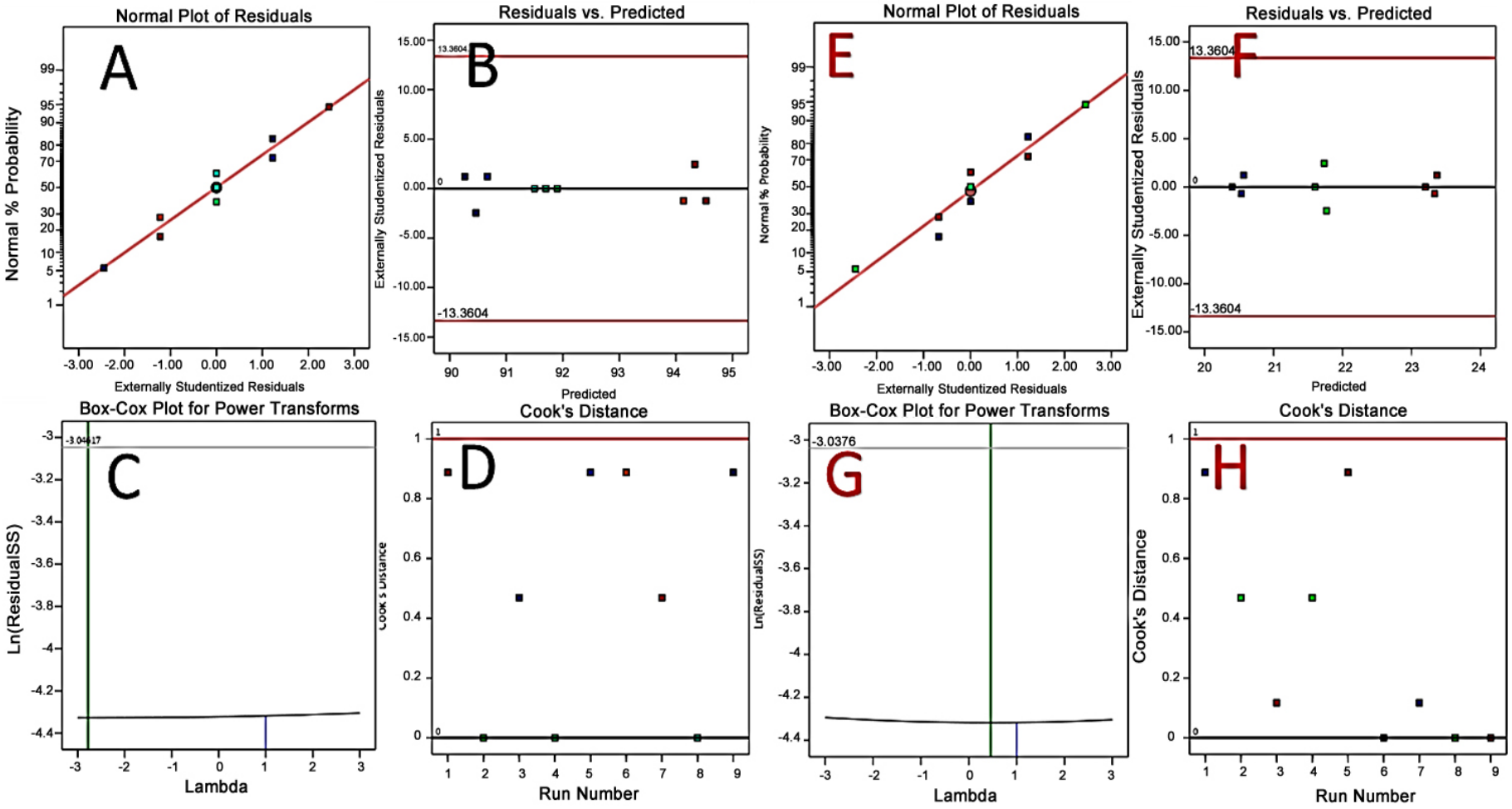

Figure 3A-H. Plots showing the interaction effect of polymers on drug released 10h and the mucoadhesive strength of AMMM

ANOVA details of the responses

Table 5 provides details of the ANOVA for DR10h. As shown in Fig. 4, the contour plot and response surface plot show the same increase in the MS of AMMM along with an increase in the amount of carbopol 934 P and MG. 9 experiments were conducted by a central composite design. The responses detected for 9 AMMM fitting to the quadratic models simultaneously with Design-Expert 11.0 software and the outcomes of the analysis of variance (ANOVA) for the selected factorial model (Table 5).

Table 5. ANOVA for Quadratic model

ANOVA for Response 1: Drug released (10h)						
Source	**Sum of Squares**	**df**	**Mean Square**	**F-value**	**p-value**	
Model	23.65	5	4.73	1064.10	< 0.0001	significant
A-Carbopol 934P	0.2400	1	0.2400	54.00	0.0052	
B-AIFM	22.43	1	22.43	5046.00	< 0.0001	
AB	0.0000	1	0.0000	0.0000	1.0000	
A^2	0.0000	1	0.0000	0.0000	1.0000	
B^2	0.9800	1	0.9800	220.50	0.0007	
Residual	0.0133	3	0.0044			
Cor Total	23.66	8				
ANOVA for Response 2: mucoadhesive strength (g)						
Model	11.89	5	2.38	534.90	0.0001	significant
A-Carbopol 934P	0.0417	1	0.0417	9.38	0.0549	
B-AIFM	11.76	1	11.76	2646.00	< 0.0001	
AB	0.0000	1	0.0000	0.0000	1.0000	
A^2	0.0050	1	0.0050	1.12	0.3667	
B^2	0.0800	1	0.0800	18.00	0.0240	
Residual	0.0133	3	0.0044			
Cor Total	11.90	8				

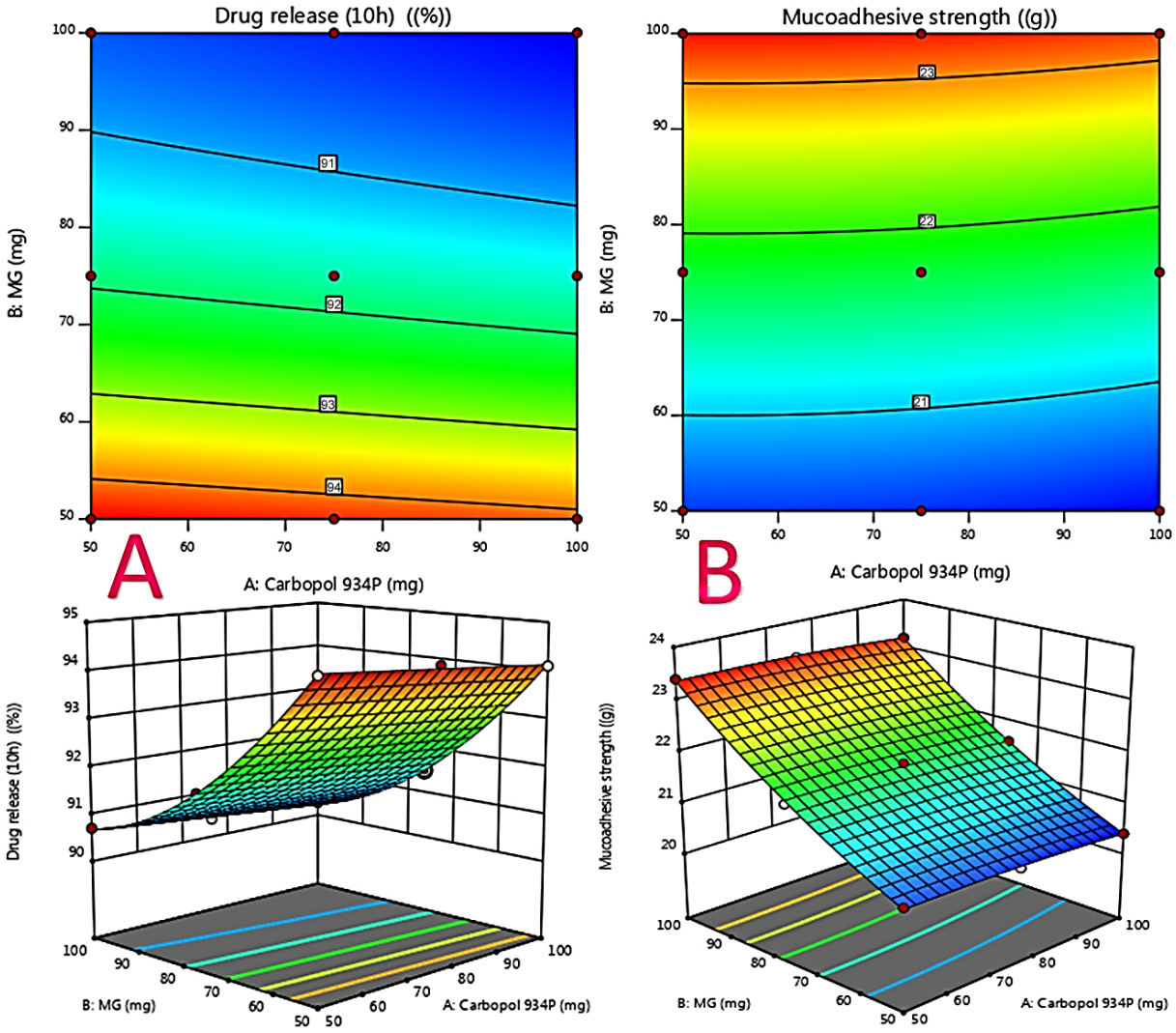

Figure 4. Contour plot and 3D response plot for DR10h (A) and mucoadhesive strength (B)

A 3D response plot for MS and a contour plot for DR10h are shown in Fig. 4.

4. Discussion

The purified MG was in yellowish green colour that indicates its purity. ATH spectrum was found to be similar with the reference and this indicates the presence of all the functional groups in the pure ATH. Additionally, the ATH melts as indicated in the monograph of Indian Pharmacopoeia.

The DSC analysis of ATH blend shifted to the left compared to the pure ATH, indicating the proper impregnation of ATH with the excipients used. ATH exhibits distinctive peaks characteristic of FTIR bands for its functional groups.

The particle size of AMMM was uniform, the % yield was >80% and the ATH entrapment was appreciable. With AMMM, mucoadhesion patterns and ATH release patterns can be derived to determine the extent of mucoadhesion. Therefore, this study should be painstaking when arranging any mucoadhesive formulations. A variety of MG concentrations were tested on the swelling indices of the AMMM. As the concentration of MG decreased, the swelling index decreased steadily. It is known that MG contains many polar compounds, which cause high water absorption and holding capacity, as well as swelling properties in AMMM.

The % mucoadhesion was dependent on the amount of MG as the higher MG content higher the mucoadhesion. The ATH release at the end of the 10h is high for the formulations F-1 and F-2, Zero order kinetics was best fit the release of ATH from the AMMM.

On the normal likelihood plot of outwardly studentized residuals, there were a maximum of colored points representing the DR10h around the normal probability line, which confirmed the normality of residuals and recommended the appropriate analysis of response data. Because there is a straight line stratified around the residuals, the normality hypothesis is satisfied (Fig. 3A). DR10h had colored points within the limits of the DR10h

plot when studentized residuals versus predicted values were depicted. This plot confirms the postulation of constant variance by illustrating the random distribution of studentized residuals (Fig. 3B). We identified the variables that may have influenced DR 10h after testing by plotting residuals versus run numbers. It was evident from all points that there were no faraway observations throughout and that the runs were steady (Fig. 3C). According to the predicted vs. actual values plot (Fig. 3D), the experimentally pragmatic values of the ATH release were close to the prophesied values.

Normal likelihood plots of superficially studentized residuals specified that most of the colored points indicating MS were observed around the normal probability line, thereby confirming the normality of residuals and recommending the appropriate analysis of response data. As the residuals are plotted around a straight line, the normality assumption is satisfied (Fig. 3E). The plot of predicted values versus residuals externally studentized revealed that MS points were within established limits. A random distribution of the studentized residuals indicates that the continuous variance hypothesized by the authors was true (Fig. 3F). We found variables that may have influenced DR10h during the study by plotting residuals versus run number. It was evident throughout that the points did not have any outlying reflections and all runs were stable (Fig. 3G). MS experimentally perceived values were close to the predicted values (Fig. 3H), as shown in the predicted vs. actual values plot.

The model F-value of 55.13 indicates that the model is significant. The probability of an F-value this large occurring due to noise is only 0.38%. Model terms that are significant are marked with <0.05 P-values. X_1, X_2 are significant model terms in this case. The values >0.1 indicate that the model terms are not significant. DR10h was coded as: DR10h =+91.70-0.2000A-1.93B+0.0000AB+0.0000A^2+0.7000B^2

For given levels of each factor, the equation based on coded factors can predict the response. Factors with high levels are automatically coded as +1 while factors with low levels are coded as -1. By comparing the coefficients of the factors, the coded equation can be used to recognize the virtual impact of the factors.

The predicted R^2 of 0.9931 is reasonably close to the adjusted R^2 of 0.9985, i.e., the difference is <0.2. Signal-to-noise ratio is determined by adequate precision. The signal must be adequate when the ratio is > 4, and the signal must be 78.384 (adequate). By using this model, the design space can be circumnavigated.

The contour plot and response surface plot show the same increase in the MS of AMMM along with an increase in the amount of carbopol 934 P and MG. Final equation in terms of coded factors for MS= +21.73-0.0833A+1.40B+0.0000AB-0.0500A^2+0.2000B^2.

For certain levels of each factor, the equation in terms of coded factors can be used to predict the response. The default coding of the factors is +1 for high levels and -1 for low levels. By comparing the coefficients of the factors, the coded equation can be used to identify the relative impact of the factors.

The predicted R^2 of 0.9821 is reasonably close to the adjusted R^2 of 0.9890, i.e., the difference is <0.2. Signal-to-noise ratio is determined by adequate precision. The signal must be adequate when the ratio is > 4, and the signal must be 54.501 (adequate). By using this model, the design space can be circumnavigated. 9 experiments were conducted by a central composite design that fit to the quadratic model.

The model F-value of 1064.10 indicates the model is significant. The probability of an F-value this large occurring due to noise is only 0.01%. Model terms with P-values of less than 0.0500 are significant. As you can see, there are three significant model terms here: A, B, and B_2. An absence of significance is indicated by values greater than 0.1000. Model reduction may be beneficial if your model contains many insignificant terms (excluding those that support your hierarchy).

The Model F-value of 534.90 indicates that the model is significant. There is only a 0.01% chance that an F-value this large could occur due to noise.

The model terms with P-values less than 0.0500 are significant. The model terms B_2 and B_3 are significant in this case. Model terms are not significant when they exceed 0.1000. Model reduction may improve your model if it contains many insignificant terms (excluding those that are required to support the hierarchy).

With the equation in terms of coded factors, it is possible to predict the response to given levels of each factor. The default coding is +1 for high levels and -1 for low levels. This equation can be used to determine whether one factor is more important than another by comparing its coefficients.

Two factors are simultaneously influencing the response to this type of plot. The contour plot and response surface plot (Fig. 4) show that an equivalent increase in the mucoadhesion time of drugs takes place with a rise in the amount of MG and Carbopol 934 P.

5. Conclusions

Mucoadhesive polymers can control the concentration and rate of Amoxicillin Trihydrate (ATH) release, thereby contributing to the therapeutic activity of mucoadhesive drug delivery systems (MDDS). ATH is released from the stomach by the retention of MDDS. Mastic gum was combined with Carbopol 934 P to manufacture nine formulations of AMMM. In comparison to other formulations, Formulations F-1 and F-2 showed a decent cumulative release of ATH after 10 h. With an increase in MG content, mucoadhesive strength was perceived to increase in all batches. In conclusion, the present study concludes that MDDS for ATH coupled with Carbopol

934 P is an efficient approach to retaining in the stomach with increased bioavailability.

Acknowledgments

The authors are thankful to the college management for providing the facilities for performing this research work.

Declaration of Competing Interest

The author declared no conflict of interest.

Author's Contribution

Sowjanya Hatthi Belgal Mundarinti performed the work, and Hindustan Abdul Ahad reviewed, revised, and arranged the work as per the journal format.

REFERENCES

[1] Badoni A, Ojha A, Gnanarajan G, Kothiyal P. Review on gastro retentive drug delivery system. The pharma innovation 2012;1:32.

[2] Shaha S, Patel J, Pundarikakshudu K, Patel N. An overview of a gastro-retentive floating drug delivery system. Asian journal of pharmaceutical sciences 2009;4:65-80.

[3] Ahad HA, Haranath C, Rahul Raghav D, Gowthami M, Naga Jyothi V, Sravanthi P. Overview on Recent Optimization Techniques in Gastro Retentive Microcapsules by Factorial Design. Int J Pharm Sci Res 2019;10:247-54.

[4] Georgopoulos A, Borek M, Ridl W, Amoxycillin Bronchitis Study Group T. Randomized, double-blind, double-dummy study comparing the efficacy and safety of amoxycillin 1 g bd with amoxycillin 500 mg tds in the treatment of acute exacerbations o f chronic bronchitis. Journal of Antimicrobial Chemotherapy 2001;47:67-76.

[5] Bittner L, Heigl N, Petter C, Noisternig M, Griesser U, Bonn G, et al. Near-infrared reflection spectroscopy (NIRS) as a successful tool for simultaneous identification and particle size determination of amoxicillin trihydrate. Journal of pharmaceutical and biomedical analysis 2011; 54:1059-64.

[6] Thombre NA, Gide PS. Floating-bioadhesive gastroretentive Caesalpinia pulcherrima-based beads of amoxicillin trihydrate for Helicobacter pylori eradication. Drug delivery 2016;23:405-19.

[7] Dey SK, De PK, De A, Ojha S, De R, Mukhopadhyay AK, et al. Floating mucoadhesive alginate beads of amoxicillin trihydrate: A facile approach for H. pylori eradication. International journal of biological macromolecules 2016;89:622-31.

[8] Raafat AI, Kamal H, Sharada HM, Mohamed RD. Radiation development of gastroretentive amoxicillin trihydrate floating-alginate based beads for the treatment of helicobacter pylori. Radiation Physics and Chemistry 2021;179:109268.

[9] Ahad HA, Sreeramulu J, Bindu VH, Kumar CS, Reddy B, Chandana RV, et al. Design and evaluation of sustained release matrix tablets of glimepiride based on combination of natural and synthetic polymers. 2010.

[10] Donnaloja F, Jacchetti E, Soncini M, Raimondi MT. Natural and synthetic polymers for bone scaffolds optimization. Polymers 2020;12:905.

[11] Dabos K, Sfika E, Vlatta L, Giannikopoulos G. The effect of mastic gum on Helicobacter pylori: a randomized pilot study. Phytomedicine 2010;17:296-9.

[12] Paraschos S, Magiatis P, Mitakou S, Petraki K, Kalliaropoulos A, Maragkoudakis P, et al. In vitro and in vivo activities of Chios mastic gum extracts and constituents against Helicobacter pylori. Antimicrobial agents and chemotherapy 2007;51:551-9.

[13] Miyamoto T, Okimoto T, Kuwano M. Chemical composition of the essential oil of mastic gum and their antibacterial activity against drug-resistant Helicobacter pylori. Natural products and bioprospecting 2014;4:227-31.

[14] Shravani Y, Ahad HA, Haranath C, gari Poojitha B, Rahamathulla S, Rupasree A. Past Decade Work Done On Cubosomes Using Factorial Design: A Fast Track Information for Researchers..(2021). Int J Life Sci Pharma Res;11:P124-35.

[15] Ahad HA, Chinthaginjala H, Priyanka MS, Raghav DR, Gowthami M, Jyothi VN. Datura stramonium Leaves Mucilage Aided Buccoadhesive Films of Aceclofenac using 32 Factorial Design with Design-Expert Software.

[16] Chinthaginjala H, Ahad HA, Bhargav E, Pradeepkumar B. Central Composite Design Aided Formulation Development and Optimization of Clarythromycin Extended-Release Tablets. Indian journal of pharmaceutical education and research 2021;55:395-406.

[17] Terpou A, Nigam PS, Bosnea L, Kanellaki M. Evaluation of Chios mastic gum as antimicrobial agent and matrix forming material targeting probiotic cell encapsulation for functional fermented milk production. LWT 2018;97:109-16.

[18] Ahad HA, kumar BP, Haranath C, Reddy KS. Fabrication and evaluation of glimepiride Ficus benghalensis fruit mucilage matrix transdermal patches. International Journal of Chemical Sciences 2009;7:2294-8.

[19] Liu Z, Lu W, Qian L, Zhang X, Zeng P, Pan J. In vitro and in vivo studies on mucoadhesive microspheres of amoxicillin. Journal of controlled release 2005;102:135-44.

[20] Saisree R, Bhanja S, Das S, Bhavana V, Sudhakar M, Panigrahi B. Formulation and Evaluation of Mucoadhesive Microspheres of Valsartan. Research Journal of Pharmacy and Technology 2019;12:669-77.

[21] Singh C, Purohit S, Singh M, Pandey BJJoddr. Design and evaluation of microspheres: A Review. 2013;2:18-27.

[22] Annepogu H, Hindustan Abdul A, Nayakanti DJTJoPS. Determining the best poloxamer carrier for

thiocolchicoside solid dispersions. 2020;17:372.

[23] Ramya CJJoPR. Novel approach in ranitidine hydrochloride effervescent oral floating technique. 2011;4:104-6.

[24] Hindustan AA, Babu UA, Nagesh K, Kiran DS, Madhavi KBJKujos, engineering, technology. Fabrication of glimepiride scientific name stramonium leaves mucilage and poly vinyl pyrrolidone sustained release matrix tablets: in vitro evaluation. 2012;8:63-72.

[25] Chinthaginjala H, Gandla CB, Challa MR, Pradeepkumar B, Ahad HAJJoYP. Formulation and in vitro evaluation of floating tablets of dicloxacillin sodium using different polymers. 2019;11:247.

[26] Raj H, Sharma A, Sharma S, Verma KK, Chaudhary AJJoDD, Therapeutics. Mucoadhesive Microspheres: A Targeted Drug Delivery System. 2021;11:150-5.

[27] Muzaffar F, Murthy NV, Paul P, Semwal R, Shivanand PJIJCTR. Formulation and evaluation of mucoadhesive microspheres of Amoxicillin trihydrate by using eudragit RS 100. 2010;2:466-70.

[28] Paul B, Adimoolam S, Javed Qureshi MJIJoPS. Development and Evaluation of Amoxicillin Loaded Carbopol 934P Mucoadhesive Microcapsules for Sustained Drug Release for H. pylori Treatment. 2019;15:61-80.